

20. MINERALOGY AND CHEMICAL COMPOSITION OF CLAY MINERALS, TAG HYDROTHERMAL MOUND¹

Anne Sturz,² Mika Itoh,² and Susan Smith³

ABSTRACT

Herein we present preliminary results of a study of the distribution and chemical composition of clay minerals in rocks recovered from the Trans-Atlantic Geotraverse (TAG) hydrothermal mound. This study is part of Leg 158 of the Ocean Drilling Program, an effort to evaluate the subsurface secondary mineral distribution and nature of alteration at the active TAG mound, located at 26°N latitude on the Mid-Atlantic Ridge. X-ray diffraction analyses and petrographic and scanning electron microscopy indicate that the clay minerals include chlorite, smectite, and a mica-like clay. Chemical analyses by flame atomic absorption spectrophotometry of clay-mineral separates and inductively coupled plasma-atomic emission spectrophotometry analyses of basalt alteration rims indicate that the chlorite and smectite have similar major-element compositions and that both clay minerals have lower SiO₂ and Al₂O₃ and higher Fe₂O₃ and MgO than bulk basalt. Cu and Zn are elevated above unaltered basalt concentrations in the smectites and chlorites and in bulk-rock alteration rims. Spatial distributions through the mound of SiO₂/Fe₂O₃, MgO, and Zn in clay minerals and alteration rims suggest that fluids circulating through the TAG mound originate from two sources: (1) a shallowly circulating fluid that is less evolved and nearer to unaltered seawater chemical composition, and (2) a deeply circulating fluid that is more evolved fluid and changed from unaltered seawater by more extensive chemical reaction with underlying basalt. Clay-mineral compositions suggest that the southeasterly and shallow central portions of the mound are influenced by a greater proportion of the shallowly circulating, less evolved fluid, and the northwesterly and deeper central portions of the mound are influenced by a greater proportion of the deeply circulating, more evolved hydrothermal fluid.

INTRODUCTION

An important objective of Leg 158 of the Ocean Drilling Program (ODP) was to investigate the subsurface mineral distribution and mode of alteration at the Trans-Atlantic Geotraverse (TAG) hydrothermal mound, at 26°N latitude on the Mid-Atlantic Ridge. As part of the post-cruise research, we performed mineralogical and chemical analyses of clay-mineral separates from rocks collected between 15 and 121 meters below the seafloor (mbsf) from three areas of the TAG mound. This part of the project addressed the following objectives:

1. To determine clay mineralogical and chemical composition;
2. To investigate whether there is a correlation between secondary silicate mineralogy and selected heavy metal concentrations;
3. To follow the transfer of selected major, minor, and trace components from the unaltered basalt into secondary silicates and evolved fluids by comparing our clay-mineral data to unaltered basalt (Smith and Humphris, Chap. 17, this volume) and the black smoker fluids (Campbell et al., 1988) presently exiting from the apex of the TAG mound; and
4. To discern the distribution of and changes in chemical composition of subsurface fluids circulating through the mound using evidence assembled from clay-mineral data.

Based on observations and data acquired from remote sensing and submersible missions prior to Leg 158 (e.g. Becker et al., 1993; Rona et al., 1993; Fujioka et al., 1994; Humphris et al., 1995; Tivey et al., 1994; and references therein), the TAG hydrothermal mound is

roughly circular, about 200 m in diameter, with its highest part about 50 m above the adjacent basalt plain (Fig. 1). The mound has several distinct regions of presently active low- and high-temperature fluid flow associated with metalliferous materials. The highest part of the mound (northwest center) is occupied by a cluster of chalcopyrite-anhydrite-rich black smoker chimneys (Black Smoker Complex) that emit >360°C fluids (Campbell et al., 1988; Von Damm, 1995). Bathymetric profiles of the mound exhibit two terraces downslope from the Black Smoker Complex that are broader and more regular to the east and south and narrower and more rugged to the north and west. The two terraces are interpreted by Tivey et al. (1994) to represent two phases of active mound growth. The upper terrace (3644 m water depth) to the southeast of the Black Smoker Complex is a broad platform with an irregular surface and relatively high heat flow. The upper terrace to the west of the Black Smoker Complex is narrower, more irregular, and is a zone of coherent relatively low heat flow considered by Becker et al. (1993) to be a region of seawater entrainment into the mound. The lower terrace (3650 m water depth) is a broad, irregular platform to the southeast of the Black Smoker Complex. About 70 m to the southeast of Black Smoker Complex and on the lower terrace, there is a region of white smokers (the Kremlin area) venting fluids with temperatures between 260° and 300°C.

Site 957

Drilling during Leg 158 completed seventeen holes (Site 957A–957Q) drilled to various depths at five locations (TAG 1–TAG 5) around the hydrothermal mound and providing northwest–southeast and north–south cross sections across the mound (Fig. 1). TAG-1 is located east of the Black Smoker Complex on the upper terrace. The combined TAG-1 holes (Holes 957C, 957D, 957E, 957F, 957G, and 957L) penetrated to 125 mbsf, the deepest penetration of the five locations. The composite depth of rocks cored at TAG-1 provide a section through the hydrothermal mound and into the stockwork zone below. TAG-2 (Holes 957A, 957B, 957H, and 957N) is located on the lower terrace east of Black Smoker Complex, in the white smoker Kremlin area, and penetrated to 54.3 mbsf. TAG-3 drilled a single

¹Herzig, P.M., Humphris, S.E., Miller, D.J., and Zierenberg, R.A. (Eds.), 1998. *Proc. ODP, Sci. Results, 158*: College Station, TX (Ocean Drilling Program).

²Marine and Environmental Studies Program, University of San Diego, 5998 Alcalá Park, San Diego, CA 92110-2492, U.S.A. asturz@acusd.edu

³Department of Geosciences, University of Houston, Houston, TX 77204-5503, U.S.A.

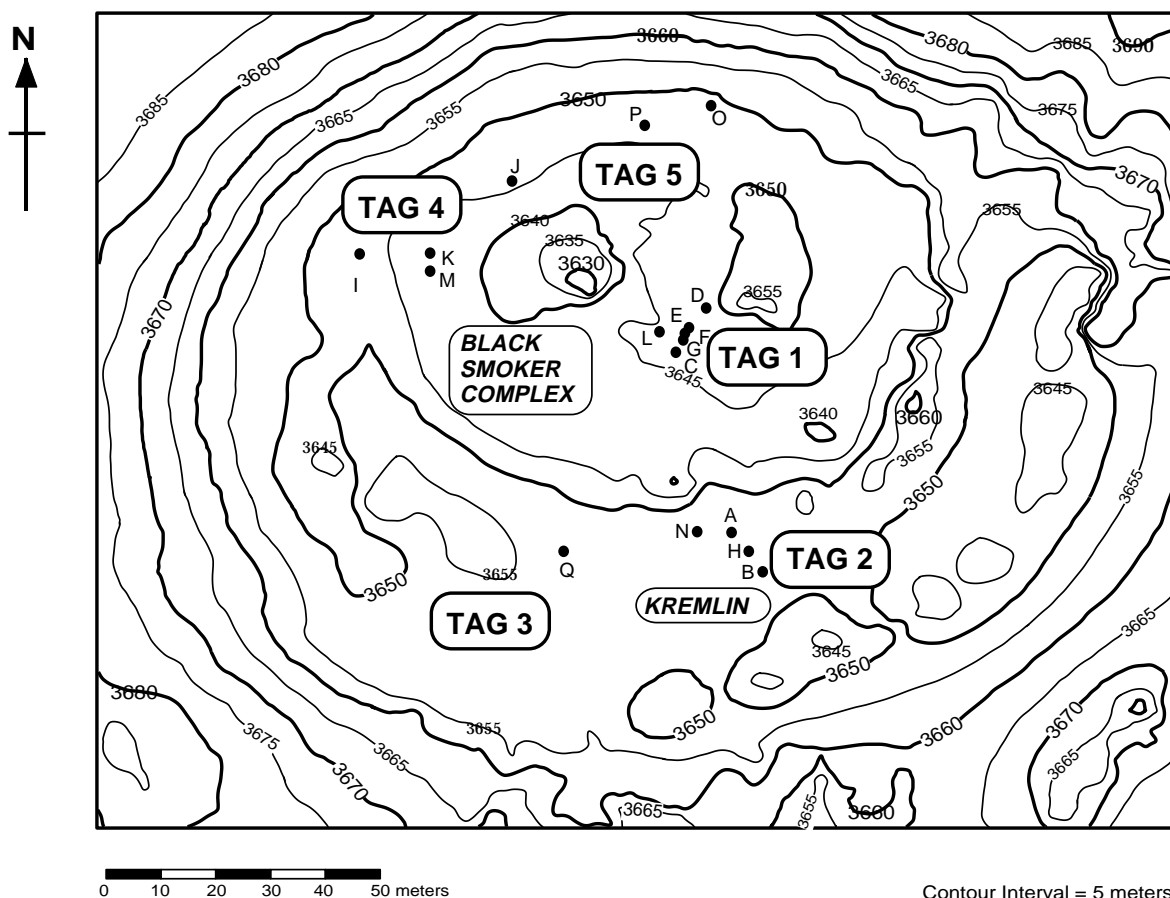


Figure 1. Topographic map of the active TAG mound showing locations of TAG-1, TAG-2, TAG-3, TAG-4, TAG-5, and the locations of Holes 957A through 957Q.

hole (Hole 957Q) to 14.5 mbsf on the lower terrace south of the Black Smoker Complex and west of the TAG-2 area. TAG-4 (Holes 957I, 957J, 957K, and 957M), located on the upper terrace on the western side of the mound, penetrated to 51.2 mbsf through mound material and into basaltic basement. Two holes (Holes 957P and 957O) on the upper terrace to the north of the Black Smoker Complex, TAG-5, had a combined penetration to 59.4 mbsf. Preliminary shipboard interpretation of cored rocks recovered by drilling at the TAG mound suggest the following stratigraphic sequence (Humphris, Herzig, Miller, et al., 1996; Fig. 2):

1. The upper few meters of the mound are dominated by porous to massive pyrite and pyrite breccias (lithology 1 in Table 1) derived from sulfide crusts, chimney talus, and near-surface hydrothermal precipitates. As much as the upper 25 m of the mound may be accumulating through primary sulfide formation and hydrothermal reworking and recrystallization to form massive sulfide breccias.
2. Below the near-surface hydrothermal precipitates is an anhydrite-rich zone that is thicker toward the interior of the mound (30 m in the TAG-1 area) than near the periphery of the mound (0–10 m in the regions of TAG 2 to TAG 5). The anhydrite-rich zone consists of pyrite-anhydrite and pyrite-anhydrite-silica breccias. Anhydrite may contribute to mound growth by subsurface deposition related to entrainment of seawater through the shallow portions of the mound.
3. Below the anhydrite-rich zone is a zone of quartz mineralization dominated by massive pyrite breccia grading to pyrite-silica breccia (lithology 2 in Table 1), grading to chloritized

basalt (lithology 3 in Table 1) and weakly mineralized basalt (lithology 4 in Table 1). The silicified breccias and chloritized basalt may represent the upper part of the stockwork zone and uppermost basement.

Local bottom water and borehole fluids were recovered using the water-sampling temperature probe (WSTP; Humphris, Herzig, Miller, et al., 1996). The borehole fluid was recovered from Hole 957C at 28.65 mbsf. Based on shipboard chemical analyses of the borehole fluid, the fluid recovered is dominated by surface seawater pumped into the hole during drilling operations. Thus, the concentrations of dissolved ions measured are artifacts of the drilling process and are not representative of the formation fluids.

Because formation fluids were not sampled during Leg 158, one objective of this study was to look for indications recorded in the clay minerals of changes in formation-fluid composition. Clay-mineral compositions were chosen for this study because they incorporate into their structure most of the major and many of the minor and trace elements contained in the original basalt. Clay minerals are very small, usually less than 4 μm in diameter, and have net negative surface charge (Brindley and Brown, 1980). Their high surface area and negative charge, providing large reaction surface and ion-exchange capacity, allow clay minerals to track relatively subtle changes in fluid chemical composition. For example, the change from low- p_e , low-pH environments of the main upflow zone to higher p_e and pH of entrained seawater in the upper part of the mound may cause decreased mobility of some trace elements, such as Fe and Zn. Such changes may be recorded in the clay minerals. Even though the analytical methods utilized in this study do not distinguish between FeO and

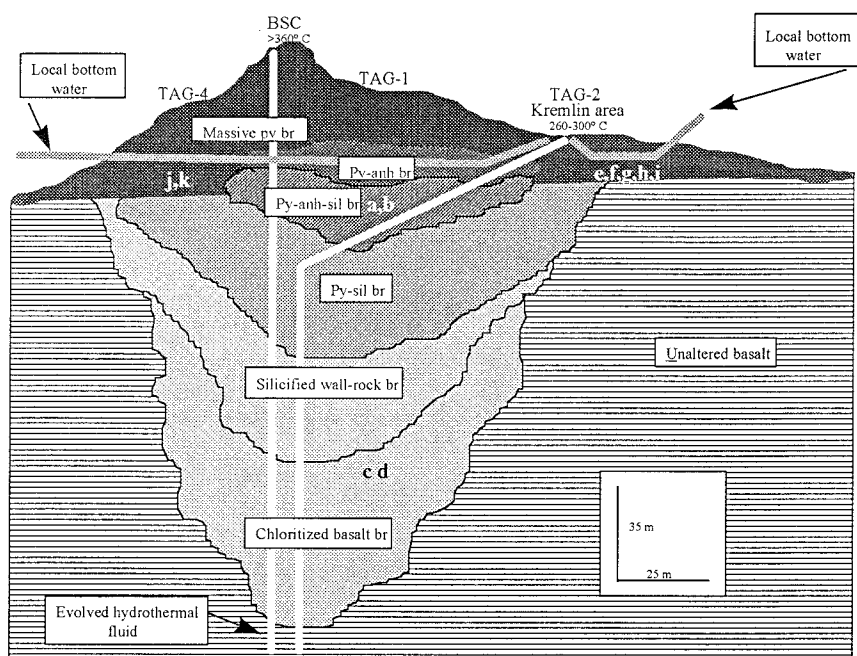


Figure 2. Schematic representation of the TAG mound, showing lithologies and fluid circulation patterns. BCS = Black Smoker Complex; py = pyrite; anh = anhydrite; sil = silica; br = breccia. Samples analyzed (designated a through n on this diagram) are identified in Table 1 (illustration by Thomas Gregory).

Fe_2O_3 , differences in total Fe, as Fe_2O_3 , incorporated into clay matrices may indicate changes in chemical environment of formation.

METHODS

Clay Sample Separation

Clay minerals were separated from the rock matrix by carefully crushing the portion of the rock of interest, followed by hand separation under a microscope and quantitative settling according to Stoke's Law of the hand-picked mineral separates to separate the <2- μm -size fraction silicate minerals from the more dense sulfides. The settled mineral separates were oven dried at 30°C for 24 hr. Mineralogical composition and relative purity of the clay-mineral separates were confirmed by inspection using a scanning electron microscope (SEM) and by X-ray diffraction (XRD) analyses of the oven dried (30°C), glycolated, and heated (350°C and 550°C) particles. The separation process was repeated until a pure clay-mineral separate was achieved.

Clay Separate Digestion and Analysis

Clay separates oven dried at (30°C) for 24 hr were dissolved using fluxed fusion of 0.02-g clay in lithium metaborate/tetraborate, and dissolution of the glass bead in 1N H_2SO_4 (Brown, 1988). Fluids were stored in polypropylene. Concentrations of major and minor components were determined as follows:

1. Silica, aluminum and titanium by standard colorimetric techniques (Brown, 1988).
2. Calcium, magnesium, potassium, sodium, copper, iron, manganese and zinc by flame atomic absorption spectrophotometry (FAAS) with reference to matched matrix aqueous standard curves for all elements measured and by direct sample standard additions for selected samples as verification of standard matrix match. It should be noted that these analyses do not distinguish between FeO and Fe_2O_3 . Thus, iron content is total Fe, as Fe_2O_3 .
3. Loss on ignition (LOI) by heating to 100°–150°C then 950°–1000°C and gravimetric determination of mass loss.

Alteration Rim Bulk Rock Analysis

Chemical analyses of basalt alteration rims were conducted by inductively coupled plasma-atomic emission spectrophotometry (ICP-AES) methods as described in Smith and Humphris (Chap. 17, this volume). These analyses were performed on bulk rock, without any attempt to separate target phases.

Results are shown in Table 1. Sample locations are shown in Figure 2.

RESULTS

Clay Mineralogy

XRD analyses indicate that five of the mineral separate samples are composed of chlorite (Table 1), as indicated by the presence of a 14-Å reflection that retains its location and magnitude through glycolation and heating. Four of the samples are composed of smectite, as indicated by the presence of a 14-Å reflection that expands to 16-Å upon glycolation and collapses to 10 Å upon heating. Some separated samples (not chemically analyzed and not shown in Table 1) had moderate to minor abundances of other clays (besides chlorite or smectite) that we identified as poorly crystalline smectite or mixed layer clays of d-spacing of 14 Å to 18 Å in the oven-dried (30°C) particles. Other separated samples (not chemically analyzed and not shown in Table 1) were composed of a mica-like clay, as indicated by the presence of a persistent 10 Å reflection throughout all treatments. The separated particles containing poorly crystalline smectite, mixed-layer clays, and the mica-like clay all were intimately intermixed with quartz and/or pyrite, and therefore were not suitable for chemical analyses using the techniques described above.

Chemical Composition of Clay Separates

Major Elements

Chlorites observed in rocks from the TAG mound are iron rich, with relatively high MgO and low SiO_2 and Al_2O_3 . Concentrations of Fe_2O_3 and MgO in the chlorites ranged from 23.9 to 40.4 wt% and 12.8 to 29.0 wt%, respectively (Table 1), which was higher Fe_2O_3 and MgO than the unaltered basalt (Smith and Humphris, Chap. 17, this

Table 1. Chemical composition of clay minerals and altered bulk rock.

Location	Hole, core, section, interval (cm)	Symbols shown in Figures 1 & 2	Mineral	Color	Depth (mbsf)	Lithology	SiO ₂	Al ₂ O ₃	Fe ₂ O ₃	MgO	Na ₂ O	K ₂ O	CaO	TiO ₂	LOI	Cu	Mn	Zn	Total	
							(wt%) ± 3.4	(wt%) ± 0.1	(wt%) ± 0.7	(wt%) ± 1.3	(wt%) ± 0.03	(wt%) ± 0.03	(wt%) ± 0.05	(wt%) ± 0.1	(wt%) ± 0.3	(mg/kg) ± 14	(mg/kg) ± 12	(mg/kg) ± 17	(wt%) ± 5.9	
TAG-1	158-957C-																			
	13N-2, 24-27	a	Smectite	Green	37.4	2	35.5	3.5	31.6	27.2	2.14	0.08	<0.1	1.3	2.1	108	803	267	103.4	
	16N-1, 28-32	b	Smectite	Green	46.5	2	37.2	4.0	29.8	24.4	2.11	0.08	<0.1	1.5	3.3	110	811	199	102.4	
	158-957E-																			
	17R-1, 1-4	c	Chlorite	Gray	116.1	3	38.5	4.4	39.9	17.2	0.17	0.11	<0.1	1.1	3.4	144	795	188	104.7	
	18R-1, 33-35	d	Chlorite	Gray	121.1	3	40.9	3.1	40.4	12.8	0.24	0.12	<0.1	1.0	3.1	130	778	180	101.6	
TAG-2	158-957B-																			
	4R-1, 28-30	e	Chlorite	Red	20.1	1	34.5	3.5	32.4	29.0	0.13	0.07	<0.1	1.4	2.7	106	835	418	103.9	
	4R-1, 39-41	f	Chlorite	Red	20.4	1	35.4	3.7	30.1	27.9	0.06	0.05	<0.1	1.5	3.3	180	779	349	101.9	
	4R-1, 55-57	g	Chlorite	Gray	20.6	1	39.9	3.7	23.9	28.4	0.09	0.04	<0.1	1.4	3.4	176	799	403	99.8	
	4R-1, 25-27	h	Bulk rock	Red		4	35.13	18.46	17.92	26.61	0.35	0.04	<0.1	2.07	10.7	19		330		
	5R-1, 4-9	i	Bulk rock	Red		4	35.41	18.87	25.29	16.41	0.51	0.03	0.35	2.02	9.26	121		207		
	4R-1, 55-62*	Basalt	Bulk rock		20.6	4	49.97	15.06	11.27	9.34	2.29	0.08	11.03	1.61	1.89	83.9		77.8		
TAG-4	158-957M-																			
	9R-1, 25-27	j	Smectite	Gray	42.6	1	38.9	3.8	43.7	14.7	1.04	0.13	<0.1	6.5	7.3	322	821	1106	110.5	
	10R-1, 96-100	k	Smectite	Gray	47.2	4	48.4	3.5	19.8	14.5	3.32	0.22	<0.1	1.2	8.1	206	1018	627	99.0	
	9R-1, 67-71	l	Bulk rock	Green		4	47.77	16.11	13.25	8.59	0.11	0.17	2.62	1.75	2.56	86.5		1572		
	10R-1, 79-74	m	Bulk rock	Red		4	48.29	15.41	12.75	9.88	2.44	0.48	8.9	1.7	3.67	71.4		345		
	10R-2, 11-14	n	Bulk rock	Green		4	42.77	17.78	19.24	10.63	2.23	0.06	4.62	1.66	5.36	108		4316		
	9R-1, 38-43*	Basalt	Bulk rock		42.8	4	50.38	15.31	10.96	8.72	2.59	0.09	10.69	1.59	1.69	78.0		98.98		
							Cl	Si	Fe	Mg	Na	K	Ca							
	local bottom water						(mmol/kg)	(mmol/kg)	(mmol/kg)	(mmol/kg)	(mmol/kg)	(mmol/kg)	(mmol/kg)							
	TAG black smoker fluid+						544	33	<0.1	54.4	476	10.5	10.3							
							659	22	1.64	0	584	17	26							

Notes: * = data from Smith and Humphris (Chap. 17, this volume); + = data from Campbell et al. (1988). Lithology: 1 = massive pyrite breccia, 2 = pyrite silica breccia, 3 = chloritized basalt, 4 = basalt.

volume). Concentrations of SiO₂, Al₂O₃, Na₂O, and CaO in the chlorites range from 35.4 to 40.9 wt%, 3.5 to 4.4 wt%, 0.24 to 0.6 wt%, and <0.1 wt%, respectively, all lower than those in the unaltered basalt (Smith and Humphris, Chap. 17, this volume). TiO₂ in the chlorites is near or less than TiO₂ in the unaltered basalt.

Chemical composition of the smectites observed in rocks from the TAG mound are similar to those observed in the chlorites, with minor differences. The smectites have a broader range of Fe₂O₃ concentrations (19.8–43.7 wt%) and a similar range of MgO concentrations (14.5–27.2 wt%). With one exception, TiO₂ in the smectites are near or less than TiO₂ in the unaltered basalt. Sample 158-957M-9R-1, 25–27 cm, has anomalously high TiO₂ relative to the other clay minerals analyzed. Concentrations of Na₂O in the smectites are very close to that of the basalt.

Trace Elements in Clay Separates

Concentrations of Cu and Zn in both the chlorites and the smectites are higher than they are in the basalts and are higher in clay samples recovered from shallower depths in the mound than those recovered from deeper in the mound (Table 1). On a mol/mol transfer of Zn from basalt into secondary silicates, Zn is enriched by as much as 400% in the TAG-4 region in the clays relative to the basalt.

Chemical Composition of Basalt Alteration Rims

Major Elements

Chemical analyses of bulk-rock basalt alteration rims verify the general trends observed in the clay-mineral separates. Alteration rims are Fe rich, with relatively high MgO and low SiO₂, compared to the unaltered basalt. For ease of handling, the alteration rims were classified by color: green or red. Concentrations of Fe₂O₃ and MgO in the green rims ranged from 13.3 to 19.2 wt% and from 8.6 to 10.6 wt%, respectively (Table 1), slightly higher Fe₂O₃ and MgO than in the unaltered basalt. Concentrations of SiO₂, Al₂O₃, Na₂O, and CaO in the green rims range from 42.7 to 47.8 wt%, 16.1 to 17.8 wt%, 2.2 to 2.4 wt%, and 2.6 to 4.6 wt%, respectively, all lower than in the unaltered basalt, but closer to values in the basalt than the clay-mineral separates described above. Concentrations of Fe₂O₃ and MgO in the red rims ranged from 12.7 to 25.3 wt% and 9.9 to 26.6 wt%, respectively (Table 1), higher than in the unaltered basalt and with a wider range of compositions than the green alteration rims. Concentrations of SiO₂, Al₂O₃, Na₂O, and CaO in the red rims range from 35.1 to 48.3 wt%, 15.4 to 18.8 wt%, 0.35 to 2.4 wt%, and <0.1 to 8.9 wt%, respectively, showing a wider range of compositions than the green rims.

Trace Elements in Basalt Alteration Rims

Concentrations of Cu in both green and red rims range from 19 to 121 mg/kg, near that of the unaltered basalt (78–84 mg/kg Cu). In the red rims, Zn ranges from 207 to 403 mg/kg, slightly higher than is observed in the basalt (78–99 mg/kg), whereas Zn in the green rims is much greater (1572–4316 mg/kg) than in both the red rims and the unaltered basalt.

Iron, Silica, and Magnesium

Of specific interest for the discussion below are relative differences in iron, silica, and magnesium contents in the clay minerals. Smectite recovered from TAG-4, the northwesterly side of the mound, (Sample 158-957M-10R-1, 96–100 cm), contains SiO₂ (48.4 wt%) and Fe₂O₃ (19.8 wt%) and is closest in silica content to that of the unaltered basalt (50.38 and 10.96 wt%, respectively; Table 1). Smectite separated from the overlying breccia (Sample 158-957M-9R-1, 25–27 cm) has lower SiO₂ (38.9 wt%) and higher Fe₂O₃ (43.7 wt%). Bulk-rock altered red rim (Sample 158-957M-10R-1, 69–74 cm) and

green rims (Samples 158-957M-09R-1, 67–77 cm, and 10R-2, 11–14 cm) contain SiO₂ (48.3, 47.8, and 42.7 wt%, respectively) and Fe₂O₃ (12.8, 13.3, and 19.2 wt%, respectively), all very close to that of the basalt.

Chlorites associated with massive pyrite breccia (Samples 158-957B-4R-1, 28–30 cm, 4R-01, 39–41 cm, and 4R-1, 55–57 cm) and red alteration rims (Samples 158-957B-4R-01, 25–27 cm, and 5R-1, 4–9 cm) are found at a relatively shallow depth at TAG-2, the southeasterly side of the mound. These chlorites contain SiO₂ (34.5, 35.4, and 39.9 wt%, respectively) and Fe₂O₃ (32.4, 30.1, and 23.9 wt%, respectively), lower silica and higher iron than observed in smectites at TAG-4 and in the basalt. The red rims contain SiO₂ (35.13 and 35.41 wt%, respectively) and Fe₂O₃ (17.92 and 25.29 wt%, respectively), also lower silica and, in Sample 158-957B-5R-1, 4–9 cm, higher iron than at TAG-4 and in the basalt.

Smectites recovered from pyrite-silica-breccia at a relatively shallow depth at TAG-1 (Samples 158-957C-13N-2, 24–27 cm, and 16N-1, 28–32 cm) contain SiO₂ (35.5 and 37.2 wt%, respectively) and Fe₂O₃ (31.3 and 29.8 wt%, respectively), similar to the chlorites from TAG-4. Chlorites recovered from the chloritized basalt, from below 115 mbsf at TAG-1, contain SiO₂ (38.5 and 40.9 wt%, respectively) and Fe₂O₃ (39.9 and 40.4 wt%, respectively), similar to the smectites from TAG-2.

It is also interesting to note that, with the exception of one red rim bulk rock sample (Sample 158-957B-5R-1, 4–9 cm) magnesium contents in the TAG-4 samples and TAG-1 samples recovered from below 115 mbsf are lower (8.59–17.2 wt%) than the magnesium contents in the TAG-2 samples and TAG-1 samples recovered above 50 mbsf (24.4–29.0 wt%; Table 1).

The smectites and alteration rims from the TAG-4 region have a narrow range of MgO contents, only slightly higher than the basalt (Table 1). The MgO contents of chlorites from the TAG-2 region also have a narrow range, but are significantly higher than the basalt. Altered rims from the TAG-2 region have a larger range of MgO contents (16.4–26.6 wt%), a range spanning those observed in the clay minerals from both regions. The smectites from the shallower region of TAG-1 are higher (27.2 and 24.4 wt% MgO) than the basalt, more similar to the MgO contents of the chlorites from TAG-2. The values of chlorites from the deeper region of TAG-1 (17.2 and 12.8 wt% MgO) are closer to that of the basalt and more similar to the smectites from TAG-4.

DISCUSSION

Based on preliminary shipboard interpretation of the lithologic sequence observed at TAG (Humphris, Herzig, Miller, et al., 1996; Humphris et al., 1995), entrainment of large quantities of local bottom water into the upper portion of the mound is an important component of fluid circulation through the mound. The shallow component of fluid circulation contributes to the mound-building process by forming large quantities of anhydrite, perhaps as much as 10⁵ m³. Lithologic units below the anhydrite breccias, deeper than about 50 mbsf and beneath the central portion of the mound, have little to no anhydrite. The deeper units are interpreted to be influenced by deeply circulating, more evolved, hydrothermal fluids. One objective of this study was to use clay-mineral chemical compositions to verify the shipboard preliminary interpretation of two sources of fluids circulating through the mound. Another objective of this study was to use authigenic clay-mineral compositions to identify regions of the mound affected by different proportions of mixing between deeply circulating, more evolved fluid, and shallowly entrained, less evolved fluid.

Formation of Fe- and Mg-bearing clay minerals, such as those observed in the TAG rocks, requires an abundant source of Fe, Mg, and SiO₂. Because the local bottom water contains less than detectable concentrations of dissolved Fe and dissolved SiO₂ near 30 μM

(Humphris, Herzig, Miller, et al., 1996), the source of Fe and SiO₂ must be the basalt. Similarly, local bottom water contains less than detectable concentrations of dissolved Zn and Cu. Therefore, enrichments of Cu and Zn observed by shipboard investigations in upper lithologic units must also be derived from the basalt. In contrast, sources of Mg can be either or both the basalt and seawater. The Kremlin area of the TAG mound is a region of white smokers with venting temperatures between 260° and 300°C (Humphris et al., 1995). Mg is quantitatively removed from seawater early in its hydrothermal evolution history when heated to this range of temperatures (e.g. Bischoff and Dickson, 1975; Bischoff and Seyfried, 1978; Von Damm, 1988). Thus, major-element composition of the fluids circulating to different depths with different evolution histories are expected to be different. Clay minerals formed in association with fluids of different circulation histories may reflect this difference. We will use Fe₂O₃/SiO₂ values and MgO and Zn concentrations in clay minerals from the TAG mound to infer variable degrees of mixing between two such different fluids in different regions and at different times during the accumulation history of the mound.

Iron and Silica

Data shown in Figure 3 suggest two distinct trends of Fe₂O₃/SiO₂ in the clay minerals. Fe₂O₃/SiO₂ of the unaltered basalt is at the intersection of the two trend lines. Smectites associated with the pyrite-silica-breccia were found at relatively shallow depths in the TAG-1 region (Samples 158-957C-13N-2, 22–27 cm, and 16N-1, 28–32 cm; designated a and b in Fig. 2). Chlorites were found below 115 mbsf at the TAG-1 region, associated with chloritized basalt (Samples 158-957E-17R-1, 1–4 cm, and 18R-1, 33–35 cm; designated c and d in Fig. 2). The line connecting clay minerals from the shallow regions of TAG-1 and from TAG-4 to the unaltered basalt has a steeper slope than the line connecting clay minerals from TAG-2 and the deeper regions of TAG-1 to unaltered basalt. Samples designated j and k (Fig. 2; Samples 158-957M-9R-1, 25–27 cm, and 10R-1, 96–100 cm, respectively), the smectites from TAG-4, cluster along the same trend as the chlorites from TAG-1, with k nearer in composition to the unaltered basalt and j nearer the TAG-1 chlorites. Samples designated e, f, and g (Fig. 2; Samples 158-957B-4R1, 20–30 cm, 4R-1, 39–41 cm, and 4R-1, 55–57 cm, respectively) cluster along the same trend as the smectites from TAG-1.

The Fe₂O₃/SiO₂ relationship observed in the red and green alteration rims is less clear. On first inspection, the Fe₂O₃/SiO₂ data

shown in Figure 3 for all the alteration rims plot along the more shallowly sloping line. However, it should be remembered that the alteration rim analyses were performed on bulk-rock samples. The presence of quartz intimately intermixed with the clay minerals would dilute the iron concentration measured and enrich the silica concentration measured relative to the clay-mineral composition, thus moving the point plotted for that sample down and to the right on the diagram.

The distinctly different trends between Fe₂O₃/SiO₂ and the basalt composition suggest that different regions of the mound have been influenced by fluids of different Fe₂O₃/SiO₂ relative ratio. The presence of abundant authigenic quartz and pyrite, as are observed in the TAG rocks, is consistent with a fluid that is chemically evolving through precipitation of secondary solids.

Magnesium

Figure 4, showing relative proportions of Fe₂O₃ and MgO in clay-mineral separates and altered rims, suggests two fields of Fe₂O₃/MgO relative ratio. (Sample designations a through n are given in Table 1 and refer to the same samples discussed above.) Samples a, b, e, f, g, and h plot in a field of relatively high MgO. The clay minerals that plot in this field were recovered from TAG-2 and from the shallow portion of TAG-1. Samples c, d, j, k, l, m, and n plot in the field of relatively lower MgO and were recovered from the deeper portion of TAG-1 and from TAG-4. One sample from TAG-2, sample i, plots in this field of relatively lower MgO. However, it should be noted that MgO and Fe₂O₃ concentrations of sample i (Sample 158-957B-5R1, 4–9 cm) were measured on bulk rock from a red alteration rim. As discussed above, the presence of quartz would dilute the measured values of major oxides other than silica.

The fields of differing Fe₂O₃/MgO suggest that chemical reactions associated with fluids circulating at shallow depths through the southeasterly side of the mound at TAG-2 and the upper portion of the central region of the mound at TAG-1 are producing clay minerals, both smectite and chlorite, with relatively high MgO contents, whereas chemical reactions associated with fluids circulating through the westerly (TAG-4) and deep central (TAG-1) portion of the mound are producing clay minerals, both smectite and chlorite, with relatively low MgO contents. Thus, TAG-4 and the deeper portion of the central part of the mound were exposed to relatively low-Mg fluids at the time the clay minerals were formed. In contrast, the TAG-2 area and the shallower portions of the central part of the mound were exposed

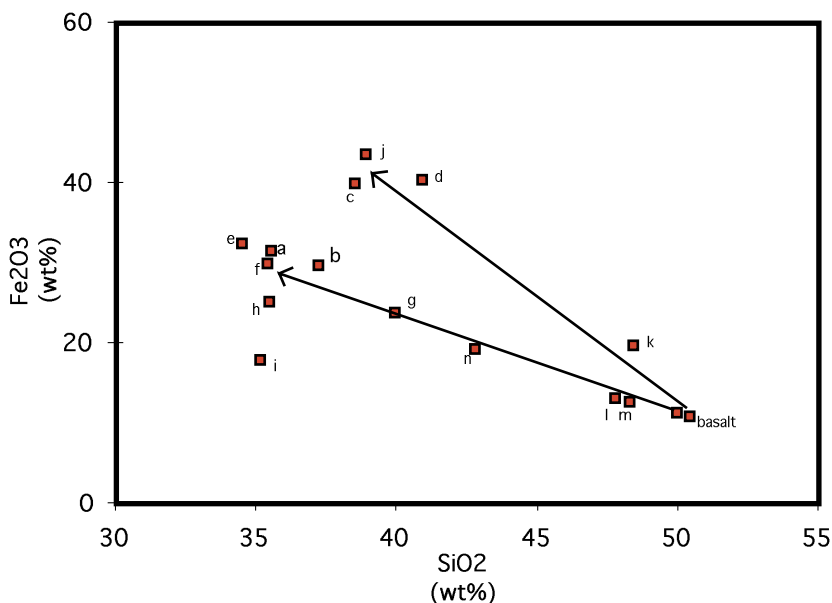


Figure 3. Weight percent SiO₂ and Fe₂O₃ in clay minerals and alteration rims. Sample identifications (a through n) are given in Table 1 and are located in Figure 2. The lines indicate trends of change in SiO₂ and Fe₂O₃ from the starting material, unaltered basalt, to the measured concentrations in the TAG clay minerals in various regions of the TAG active hydrothermal mound. The more shallowly sloping line shows the trend observed for TAG-2 and the shallower region of TAG-1. The more steeply sloping line shows the trend for TAG-4 and the deeper region of TAG-1.

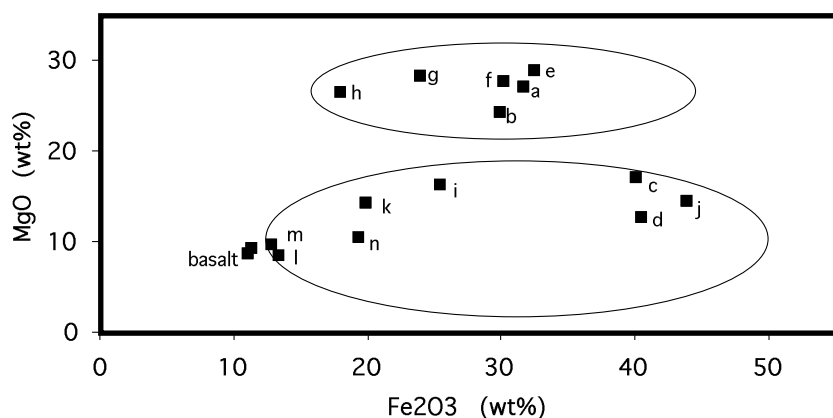


Figure 4. Weight percent Fe_2O_3 and MgO in clay minerals and alteration rims. The group of samples with relatively high MgO content (a, b, e, f, g, and h in the upper ellipse) are from the shallower region of TAG-1 and from TAG-2. The group of samples with relatively low MgO content (c, d, i, j, k, l, m, and n in the lower ellipse) are from the deeper region of TAG-1 and from TAG-4.

to more Mg-enriched fluids during the episode(s) of clay-mineral formation.

Zinc

Another important finding is that Zn concentrations in smectite and chlorite are higher around the margins of the mound (TAG-2 and TAG-4) than in the central portion of the mound and that the red alteration rims have lower Zn content than the green rims (Table 1). The highest Zn concentrations were measured in the TAG-4 area. Zinc in the chlorites and smectites from the TAG-1 region are relatively low, with the highest Zn concentrations in this region found in the shallowest samples. Therefore, those regions with clay minerals that are relatively enriched in Zn are the peripheral regions of the mound, generally associated with the massive pyrite breccia and interpreted to be chimney talus (Humphris et al., 1995). The variability in Zn concentrations associated with clay minerals may represent differences in dissolved Zn in circulating fluids. The variation in Zn associated with different colors of the alteration rims also implies specific fluid zones. This is consistent with the shipboard interpretation that Zn has been remobilized during late-stage circulation of fluids and reprecipitated as sphalerite-rich chimneys and domes (Humphris, Herzig, Miller, et al., 1996).

Mixing of Fluids from Different Sources

The observed distributions of $\text{Fe}_2\text{O}_3/\text{SiO}_2$, MgO , and Zn in chlorites and smectites from the TAG mound are consistent with two fluid sources, one more evolved fluid from a high-temperature reaction zone at depth, and the other local bottom water entrained into shallow portions of the mound and less evolved than the deeply circulating fluid. These data suggest that mixing of the two fluids within the mound is not uniformly distributed. Locally derived, less evolved water has a larger influence on the clay minerals formed in the southeastern TAG-2 and shallow central TAG-1 regions than in other parts of the mound. This is consistent with measured exit temperatures of present-day fluids ($260^\circ\text{--}300^\circ\text{C}$) at the TAG-2 region (Campbell et al., 1988; Humphris et al., 1995, and references therein).

In contrast, the clay minerals recovered from the deeper central portion of the mound were formed in association with a greater proportion of more evolved hydrothermal fluids. This is consistent with the fluids presently exiting with temperature in excess of 360°C from the apex of the mound at the Black Smoker Complex (Campbell, et al., 1988; Humphris et al., 1995, and references therein). Based on the clay-mineral composition in the shallow portions of TAG-1, fluids presently exiting at the Black Smoker Complex must pass rapidly through the talus mound with little loss of dissolved components into clay minerals. The clay minerals from the shallow regions of TAG-1 analyzed during this project were apparently derived from an episode of clay formation from fluids more similar to those presently exiting

from the TAG-2 region (that is, fluids derived from mixing a greater proportion of less evolved fluids with a lesser proportion of more evolved fluids).

Interpretation of the TAG-4 region data is more ambiguous. Becker et al. (1993) suggest that the northwesterly side of the TAG mound is a region of relatively low heat flow, perhaps a zone of bottom-water entrainment into the mound. However, the clay-mineral data reflect authigenic mineral formation from a more evolved fluid, perhaps similar to that presently exiting from the Black Smoker Complex and influencing the deeper portions of the central mound. Also, Zn contents in the clay minerals and green alteration rims from the TAG-4 region are more consistent with a fluid relatively high in dissolved Zn. Such discordance between trace- and major-element chemical composition may be explained in terms of the role a trace element, such as Zn, may play in the clay-mineral structure. Zinc may not reside in a major structural site in the clay mineral (Brindley and Brown, 1980). Whereas the major-element composition (SiO_2 , Fe_2O_3 , MgO) of the clay mineral reflects the composition of the fluid as the mineral is forming, the Zn may be acquired from a different composition fluid, through ion exchange at any time after the mineral has formed. The contrast of major- and trace-element clay-mineral chemical composition at TAG-4, as well as the association between Zn and alteration color, implies multiple episodes of fluid circulation.

Based on the chemical composition of clay minerals at the TAG mound, it is clear that construction of the mound and formation of authigenic minerals results from mixing of fluids from two different sources. Mixing between the two fluids in the subsurface is variable in time and space. The present-day venting fluid compositions do not account for the observed clay-mineral composition. Comparison of clay-mineral compositions from the central portion of the mound and the southeasterly portion of the mound suggests that the shallow central and southeasterly portions of the mound have been exposed to fluids derived from a mixture of locally entrained bottom water and deeply circulated, highly evolved hydrothermal fluid. The deep central portions of the mound have been exposed to a greater proportion of more evolved hydrothermal fluids. Fluids circulating through the northwesterly portion of the mound may have been hotter in the past than they are now.

CONCLUSIONS

1. Clay minerals separated from rocks recovered during Leg 158 at the TAG hydrothermal mound consist of chlorite and smectite. A mica-like clay and mixed-layer clays are also present, but in considerably lesser amounts.
2. The concentrations of SiO_2 , Fe_2O_3 , MgO , and Zn are different in various regions of the mound, reflecting differences in the composition of the fluid from which they formed.

3. Clay minerals in the shallow portions of the central mound and the southeasterly portion of the TAG mound reflect a greater proportion of mixing between a locally derived, less evolved fluid and a deeply circulating, more evolved hydrothermal fluid.
4. Clay minerals in the deeper portion of the central mound and the northwesterly portion of the mound reflect fluids with a greater proportion of highly evolved hydrothermal fluid.

ACKNOWLEDGMENTS

We gratefully acknowledge financial support provided by USSSP for this work. Thanks, also, to Dr. Joris Gieskes of Scripps Institution of Oceanography, an anonymous reviewer, and the ODP Editorial Review Board for valuable constructive criticism that improved this manuscript.

REFERENCES

- Becker, K., Von Herzen, R.P., and Rona, P.A., 1993. Conductive heat flow measurements using *Alvin* at the TAG active hydrothermal mound, MAR at 26°N. *Eos*, 74 (Suppl.):99.
- Bischoff, J.L., and Dickson, F.W., 1975. Seawater-basalt interaction at 200°C and 500 bars: implications for origin of seafloor heavy metal deposits and regulation of seawater chemistry. *Earth Planet. Sci. Lett.*, 25:385–397.
- Bischoff, J.L., and Seyfried, W.E., 1978. Hydrothermal chemistry of seawater from 25°C to 350°C. *Am. J. Sci.*, 278:838–860.
- Brindley, G.W., and Brown, G. (Eds.), 1980. *Crystal Structures of Clay Minerals and Their X-ray Identification*. Mineral. Soc. London Monogr., 5.
- Brown, T., 1988. Wet chemical analysis of marine sediments: Applications to hydrothermal sediments of the Guaymas Basin [Master's thesis]. San Diego State Univ.
- Campbell, A., Klinkhammer, J., Palmer, M., Bowers, T., Edmond, F., Lawrence, J.R., Casey, C., Thompson, G., Humphris, S., Rona, P., and Karson, J., 1988. Chemistry of hot springs on the Mid-Atlantic Ridge. *Nature*, 335:514–519.
- Fujioka, K., Von Herzen, R.P., and the Shipboard Scientific Party, 1994. Shinkai-Yokosuka MODE '94 Leg 2 Cruise Summary: studies of an active hydrothermal mound at the TAG area on the Mid-Atlantic Ridge. *Interridge News*, 3:21–22.
- Humphris, S.E., Herzig, P.M., Miller, D.J., Alt, J.C., Becker, K., Brown, D., Brüggemann, G., Chiba, H., Fouquet, Y., Gemmel, J.B., Guerin, G., Hannington, M.D., Holm, N.G., Honnorez, J.J., Itturino, G.J., Knott, R., Ludwig, R., Nakamura, K., Petersen, S., Reysenbach, A.-L., Rona, P.A., Smith, S., Sturz, A.A., Tivey, M.K., and Zhao, X., 1995. The internal structure of an active sea-floor massive sulphide deposit. *Nature*, 377:713–716.
- Humphris, S.E., Herzig, P.M., Miller, D.J., et al., 1996. *Proc. ODP, Init. Repts.*, 158: College Station, TX (Ocean Drilling Program).
- Rona, P.A., Hannington, M.D., Raman, C.V., Thompson, G., Tivey, M.K., Humphris, S.E., Lalou, C., and Petersen, S., 1993. Active and relict sea-floor hydrothermal mineralization at the TAG hydrothermal field, Mid-Atlantic Ridge. *Econ. Geol.*, 88:1987–2013.
- Tivey, M., Humphris, S.E., Thompson, G., Hannington, M.D., and Rona, P.A., 1994. Deducing patterns of fluid flow and mixing within the TAG active hydrothermal mound using mineralogical and geochemical data. *J. Geophys. Res.*, 100:12527–12555.
- Von Damm, K.L., 1988. Systematics of and postulated controls on submarine hydrothermal solution chemistry. *J. Geophys. Res.*, 93:4551–4561.
- , 1995. Controls on the chemistry and temporal variability of sea-floor hydrothermal fluids. In Humphris, S.E., Zierenberg, R.A., Mullineaux, L.S., and Thomson, R.E. (Eds.), *Seafloor Hydrothermal Systems: Physical, Chemical, Biological, and Geological Interactions*. Am. Geophys. Union, 91:222–247.

Date of initial receipt: 31 May 1996

Date of acceptance: 10 January 1997

Ms 158SR-221